Adsorption 11: 5–13, 2005

Molecular Modeling of Adsorption in Activated Carbon: Comparison of Monte Carlo Simulations with Experiment

JIN-CHEN LIU AND P.A. MONSON*
Department of Chemical Engineering, University of Massachusetts, Amherst, MA 01003, USA

Received July 8, 2004; Revised October 14, 2004; Accepted November 3, 2004

Abstract. We present Mont Carlo computer simulation results for a molecular model of fluids adsorbed in porous carbon materials. The model carbon used is based on the platelet model for carbon of Segarra and Glandt (1994). The model we use has a single basal plane per platelet and the structure is isotropic, disordered, with weak short-range correlations between the platelets. We have performed grand canonical Monte Carlo simulations of the adsorption isotherms for methane, ethane, and their mixtures in this model carbon. We find generally good agreement with experimental and the mixture results are quite accurately described by the ideal adsorbed solution theory. An exception to this is the behavior for the mixture at the highest pressures. In this case the experimental data show significant deviations from ideal adsorbed solution theory and the simulation results.

Keywords: activated carbon, platelet model, Monte Carlo simulation, methane, ethane

1. Introduction

Activated carbon continues to be one of the most important porous materials for adsorption applications because of its high surface area and large adsorption capacity as well as low cost. Nevertheless it remains one of the most difficult systems to address with molecular modeling techniques (Bandosz et al., 2003). Through application of various experimental techniques such as high energy X-ray scattering, neutron diffraction, and high-resolution electron microscopy (HREM) the structure of activated carbon has been shown to be disordered and isotropic (Szczygielska et al., 2001a; Harria et al., 2000; Harria and Tsang, 1997) but the detailed atomic structure is still poorly understood (Harria, 1997).

The most commonly used molecular model for porous carbon is the slit-pore model (Bandosz et al., 2003), which is based on the experimental observation of short- and intermediate-range ordered structure in porous carbon. In this model, the structure of porous carbon is represented by a collection of slit shape pores with different pore widths and characterized by the pore size distribution. Although the slit pore model is the simplest and convenient to use, it ignores the edge effects, pore connectivity, the possibility of other pore shapes and other factors that have a significant influence on the adsorption behavior of disordered porous materials.

There have recently been efforts to build models for porous carbons that include the atomistic detail of the materials. These include the chemically constrained model by Acharya et al. (1999) and the model by Gubbins and co-workers (Thomson and Gubbins, 2000; Pikunic et al., 2003) based on reverse Monte Carlo method of analyzing experimental strutural data. Both these types of models were constructed in the atomic level by matching the experimental information such as C-C radial distribution function. A detailed review of these approaches is given by Bandosz et al. (2003). A difficulty for this approach is whether the structural data from experiment is sufficient to discriminate among different atomistic arrangements in the materials.

The modeling approach we have investigated here represents a middle ground between the slit pore model and the fully atomistic models of carbon and is an

extension of a model developed by Segarra and Glandt (1994). The Segarra and Glandt (1994) model treats an activated carbon as an isotropic collection of three dimensional circular platelets, each consisting of two graphitic basal planes. The thickness of each platelet was taken as 0.335 nm, and three radius values, 0.50, 0.75, 1.0 nm, were considered. The final adsorbent structure was that of three-dimensional hard platelets in thermodynamic equilibrium, generated by canonical Monte Carlo simulation of the collection of hard core platelets. This platelet model for activated carbon does capture some heterogeneous features of microporous carbon, i.e., edge effects, pore connectivity, and different pore shapes. On the other hand it neglects the atomic structure of the graphene planes in real carbons as well as other potentially important factors such as the polydispersity of the platelet size. Nevertheless, it goes well beyond the slit pore approach in realism without the complexity of the fully atomistic approaches. In this work, we suggest a modified version of the Segarra-Glandt model and use it to investigate the adsorption of methane, ethane and their binary mixtures in activated carbon via grand canonical ensemble Monte Carlo (GCMC) simulations. We compare the results with experimental data as well as the predictions of the ideal adsorbed solution (IAS) theory (Myers and Prausnitz, 1965).

2. Molecular Models, Simulation Techniques, and IAS Theory

2.1. Platelet Model for Activated Carbon

In Segarra and Glandt's platelet model, each platelet consists of two basal graphite planes and the thickness of the platelet was set to 0.335 nm, which is the distance between layers in pure graphite. From experiments, the structure of activated carbon is composed of disordered and isotropic graphite-like layers, with very weak interlayer correlations (Szczygielska et al., 2001a; Harria et al., 2000; Harria and Tsang, 1997). The fragments of the layers are approximately 1.0–5.0 nm in length (Harria and Tsang, 1997), with interlayer spacing of 0.337–0.36 nm (Szczygielska et al., 2001a, 2001b; Franklin, 1951). On the basis of this information, we have modified the Segarra-Glandt model. The physical properties for our version of the platelet model are summarized in Table 1. We use a single basal plane for each platelet, and the thickness of the platelet is chosen to be 0.335 nm. The diameter of the platelet depends on the kind of activated carbon to be modeled. In this work we seek to model BPL activated carbon, for which it has been estimated that the average plane diameter is 1.7 nm (Wolff, 1958). The particle density of the model carbon was adjusted to produce the best agreement between GCMC simulation and experimental adsorption isotherm for methane adsorbed in BPL carbon at 301.4 K. By doing so, the particle density was found to be 0.88 g/cm^3, slightly higher than the particle density of BPL carbon (0.872 g/cm^3) (Sircar and Kumar, 1986). The particle density for our model is taken to be the carbon density of the platelets (assumed to be the density of graphite) multiplied by the volume fraction of the platelets in the system. The pore volume was determined by a Monte Carlo integration technique (Myers and Monson, 2002) at $T = 298$ K, and the surface area is determined by the procedure described by Thomson and Gubbins (2000).

Table 1. Physical properties of model carbon and BPL carbon (experiments).

	Revised platelet model for carbon	Experimental
Diameter of platelet (nm)	1.7	1.7 (Wolff, 1958)
Particle density (g/cm^3)	0.88	0.872 (Sircar and Kumar, 1986)
Pore volume (cm^3/g)	0.467 (4)	0.46–0.50 (Bradley and Rand, 1995)
Surface area (m^2/g)	990 (47)	988–1120 (Reich et al., 1980; Barton et al., 1998; MacDonald et al., 2000; MacDonald and Evans, 2002)

We use 108 platelets in our model carbon in periodic boundaries, with the system volume of 212.14 nm^3. The platelet configuration was obtained from canonical Monte Carlo simulation with hard core interactions between the platelets. Figure 1 shows a computer graphics visualization of the model carbon. Figure 2 shows the radial distribution function, $g(r)$, and orientational correlation function, $g_2(r)$, for the hard platelet system. Unlike the RDF of Segarra and Glandt's platelet model, the new model has two peaks before the large peak around r equal to the diameter of the platelet. This indicates that there are weak correlations between platelets within the range of platelet diameter, corresponding to what has been found in experiments.

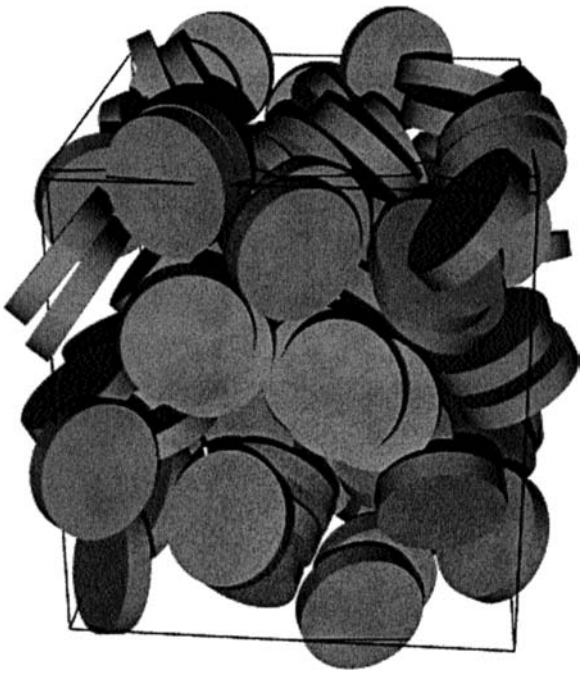

Figure 1. Computer graphics visualization of the revised platelet model for carbon.

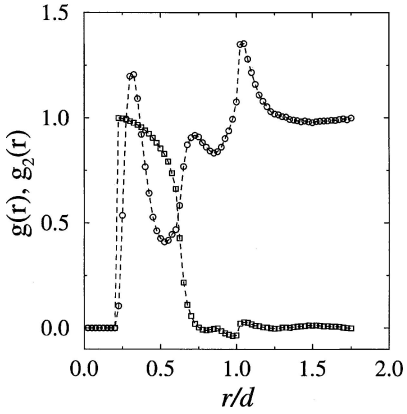

Figure 2. Radial distribution function and orientational correlation function for hard platelet system. Circles: $g(r)$; Squares: $g_2(r)$.

2.2. *Intermolecular Potentials*

Segarra and Glandt (1994) have generalized the well-known 10-4 potential for infinite carbon planes (Steele, 1973) to finite size disk layers to obtain the interaction potential between a Lennard-Jones center and a single basal platelet. We use this potential to compute the fluid-solid interaction. The interaction parameter σ_{sf} for methane and ethane was obtained by using the Lorentz-Berthelot combining rule. The parameter ϵ_{sf} was obtained by computing the Henry's constant averaged over three different realizations of the platelet structure and adjusting ϵ_{sf} to optimize the agreement with estimates of the Henry's constant from experimental adsorption isotherm data (Reich et al., 1980).

Table 2. Intermolecular potential parameters used for methane and ethane.

Species	σ_{ff} (nm)	Bond length (nm)	ϵ_{ff}/k (K)	σ_{sf} (nm)	ϵ_{sf}/k (K)
Methane	0.390	–	154.8	0.365	65.8
Ethane	0.385	0.154	105.0	0.3625	55.7

Methane was modeled as spherical Lennard-Jones molecule and ethane was modeled as two-center Lennard-Jones molecule. The fluid-fluid interaction parameters for each component were those for bulk fluids. These were chosen such that the second virial coefficients for bulk fluids agree well with the experimental values in the temperature range we studied. For this purpose, we re-parameterized the diameter of ethane (Vuong, 1998) from 0.381 nm to 0.385 nm and keep the interaction well depth unchanged. For methane, the LJ parameters were those used in the work of Kaminsky and Monson (1991). The cross interaction parameters were obtained by using Lorentz-Berthelot combining rules. The parameters used in this work are summarized in Table 2. The fluid-fluid intermolecular potential was truncated at 2.5 and 2.9 σ_{ff} for methane and ethane respectively, and fluid-solid interaction potential was truncated at half of the simulation box.

2.3. *Simulation Techniques*

We have used the conventional GCMC simulation technique (Allen and Tildesley, 1987) in this work. For GCMC simulation, we need the chemical potential instead of pressure as one of the inputs in the simulation. The Lennard-Jones 12-6 equation of state (Johnson et al., 1993) with a correction of the effect of the truncation (Finn and Monson, 1989) was used to obtain the relationship between the bulk pressure and the chemical potential for methane. For ethane and ethane-methane mixtures, we performed isothermal, isobaric ensemble Monte Carlo simulations, and the relationship between the bulk pressure and chemical potential for ethane in pure fluid and ethane/methane in mixtures were obtained by the Widom test particle method (Widom, 1963; Shing, 1985).

For calculation of the adsorption isotherm, we started from an empty matrix of solid and then performed simulations by successively increasing the chemical potential. Each subsequent simulation was started by employing the final configuration of the previous one. Simulations were run for 6×10^6, 12×10^6, and 10×10^6 configurations totally for methane, ethane, and methane-ethane mixtures respectively, with half of the configurations for equilibration. A configuration is an attempted translation, rotation (for ethane only), creation, or destruction of a molecule. For the case of methane-ethane mixtures there is also an attempted swap of the particle species of a molecule (Cracknell et al., 1993). In each case the moves were chosen with equal probability. For comparison with experimental adsorption isotherms, we need to convert the absolute adsorption obtained by GCMC simulation to excess adsorption, the quantity determined in experimental measurements. The method proposed by Myers and Monson (2002) was used for this purpose.

2.4. Ideal Adsorbed Solution Theory

IAS theory (Myers and Prausnitz, 1965) uses the principles of solution thermodynamics to describe adsorption equilibria and extends the concept of an ideal solution to such systems. The theory can be used estimate multicomponent adsorption by using only pure component data with no adjustable parameters. Following recent work we formulate the theory in terms of the total adsorption rather than the adsorption excess (Cracknell and Nicholson, 1995; Vuong and Monson, 1996). We refer the reader to the paper by Vuong and Monson (1999) for details of the implementation of IAS that we have used.

3. Simulation Results and Comparison with Experiments

3.1. Pure Component Adsorption Isotherms

Figure 3 shows the comparison of the adsorption isotherms from GCMC simulations of the model with experimental data for methane adsorption in BPL carbon at three temperatures. For simulation results, we show the isotherms for three different realizations of model carbon to see the effect of realizations on adsorption isotherms. The simulations agree very well with the experimental data for the whole range of pressures

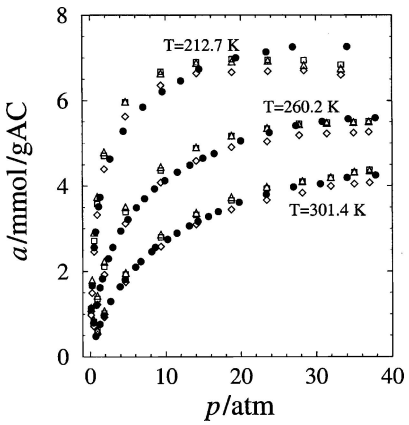

Figure 3. Comparison of adsorption isotherms calculated by GCMC simulation with Reich's experimental data for methane adsorbed in BPL carbon. Empty squares, diamonds, and triangles: MC results for different realizations of model carbon. Filled circles: experimental data (Reich et al., 1980).

up to 38 atm at high temperatures of 260.2 and 301.4 K. For the lowest temperature of 212.7 K, the simulations overestimate the adsorption isotherm at moderate pressures while underestimating the adsorption isotherms at high pressures. The appearance of the slight maximum in the adsorption excess from simulation is a common feature of supercritical adsorption isotherms for higher pressures. Figure 4 shows corresponding results for ethane. Generally the simulation results for ethane adsorption isotherms agree very well with experimental data, somewhat overestimating the adsorption isotherms at moderate pressures. Considering the parameters for our model carbon were obtained by optimizing agreement between simulation and experimental adsorption isotherm of methane at $T = 301.4$ K,

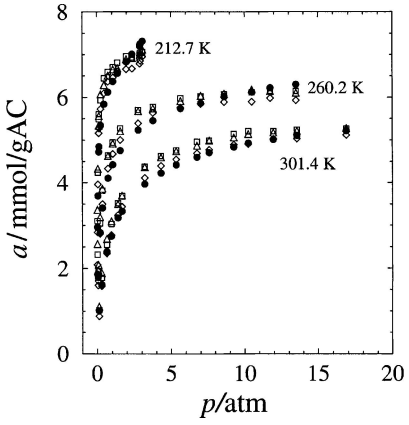

Figure 4. Same as Fig. 3 but for ethane.

it is welcome that we can also get quite good agreement for ethane adsorption isotherms as well as for methane isotherms at lower temperatures with these same parameters. Our version of the model seems to give somewhat better agreement with experiment for methane than the original model of Segarra and Glandt (1994). We were unable to reproduce the results presented for methane adsorption in activated carbon in the Segarra-Glandt paper using the parameters as described there.

It is interesting to compare our simulation results with of experimental data from different sources. Figures 5 and 6 show the comparison between simulations and experimental data by Reich et al. (1980) and Jensen et al. (1997) for methane and ethane adsorption in BPL carbon. Generally speaking, the experimental data by Reich et al. (1980) and by Jensen et al. (1997) for methane adsorption isotherms coincide with each other, although the adsorption isotherm by Jensen et al. at $T = 308.15$ K is slightly higher than that by Reich et al. at $T = 301.4$ K. Thus our simulation results also agree with the Jensen et al. data. However for ethane the discrepancies between the two sets of experimental data are quite large. The adsorption isotherms at $T = 308.15$ and 333.15 K by Jensen et al. are similar to those $T = 260.2$ and 301.4 K, respectively, by Reich et al. The reasons for these differences are not entirely clear. Certainly we should anticipate differences in the results from different samples of BPL carbon, especially given the difference in time between the two experimental studies. This illustrates one of the hazards of making quantitative comparisons of molecular simulation results with experimental data for adsorption in porous materials where the porous material microstructure is both heterogeneous and poorly characterized.

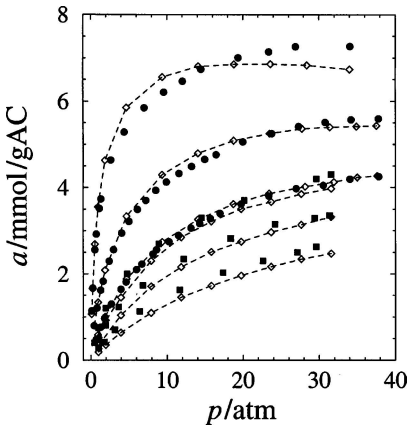

Figure 5. Comparison of adsorption isotherms calculated by GCMC simulation with experimental data by different authors for methane adsorbed in BPL carbon. Empty diamonds: MC results of averaging over three realizations of model carbon, from top to bottom: $T = 212.7$ K, $T = 260.2$ K, $T = 301.4$ K, $T = 308.15$ K, $T = 333.15$ K, and $T = 373.15$ K. The dotted lines are guides to the eye. Filled circles: experimental data by Reich et al. (1980), from top to bottom: $T = 212.7$ K, $T = 260.2$ K, $T = 301.4$ K. Filled squares: experimental data by Jensen et al. (1997), from top to bottom: $T = 308.15$ K, $T = 333.15$ K, $T = 373.15$ K.

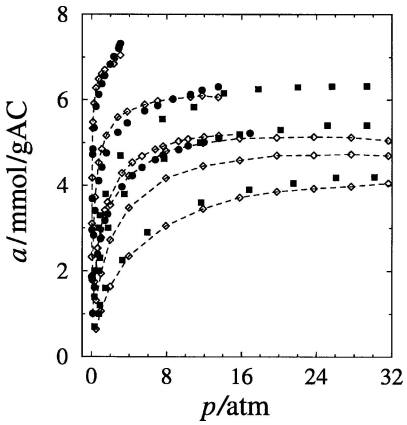

Figure 6. Same as Fig. 5 but for ethane.

3.2. *Binary Mixture Adsorption*

We also performed GCMC simulations for methane-ethane mixtures and compare with IAS theory and experimental data. In applying IAS theory, we have made two sets on calculations: one using the pure component isotherms from experiment and the other using pure component isotherms from GCMC simulations. In this way we can test the accuracy of IAS within the context of the experimental data and also within the context of the model system. Figures 7–9 show the component adsorption isotherms and *x-y* composition curves at $T = 212.7$ K from experiment and simulation together with the predictions of both implementations of IAS theory. Figure 7 shows the pressure dependence of component adsorptions for a fixed bulk composition. The agreement between simulation and experiment is very good except that the simulation results overestimate the ethane adsorption at lower pressures. IAS theory describes both the experimental and simulation results very accurately. Figure 8 shows the bulk composition dependence of the component adsorptions for a fixed bulk pressure. Again we see that the simulation results for methane agree somewhat better with experiment than those for ethane. For this

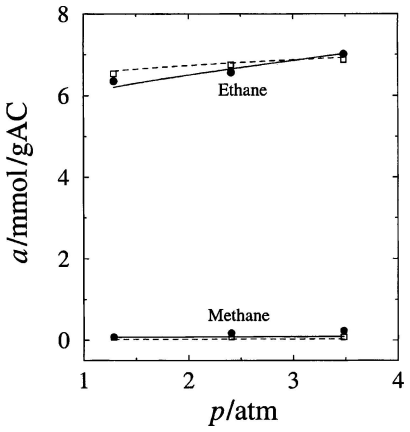

Figure 7. Component adsorption isotherms for 26.7% methane, 73.3% ethane mixtures in BPL carbon from Monte Carlo simulation, IAS theory, and experiment at $T = 212.7$ K. Filled circles: experiment (Reich, 1980); Empty squares: MC simulation results of averaging over three realizations of model carbon; Solid lines: IAS theory using experimental pure component isotherms; Dash lines: IAS theory using MC simulation pure component isotherms.

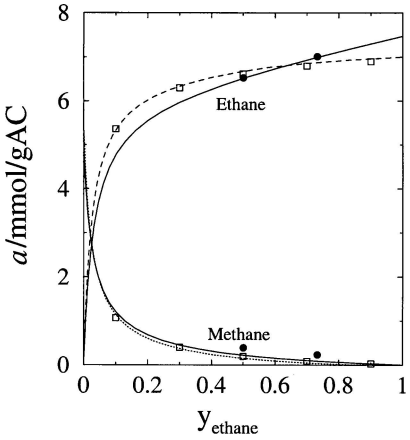

Figure 8. Component adsorption isotherms for methane-ethane mixtures in BPL carbon from Monte Carlo simulation, IAS theory, and experiment at $T = 212.7$ K and $P = 3.40$ atm. Filled circles: experiment (Reich, 1980); Empty squares: MC simulation results of averaging over three realizations of model carbon; Solid lines: IAS theory using experimental pure component isotherms; Dash lines: IAS theory using MC simulation pure component isotherms.

temperature, the simulation results overestimate the experimental data for the adsorption isotherms for ethane at low to moderate pressures and low concentrations of ethane, and underestimate the adsorption isotherms at relatively high pressures and high concentrations of ethane. This is easily understood from comparison of the simulations and experiment for the pure component adsorption isotherm of ethane at 212.7 K (see Fig. 6).

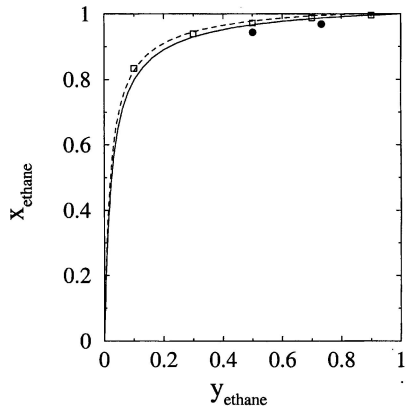

Figure 9. Comparison of *x-y* composition curves for methane-ethane mixtures in BPL carbon from Monte Carlo simulation, IAS theory, and experiment at $T = 212.7$ K and $P = 3.40$ atm. Filled circles: experiment (Reich, 1980); Empty squares: MC simulation results of averaging over three realizations of model carbon; Solid lines: IAS theory using experimental pure component isotherms; Dash lines: IAS theory using MC simulation pure component isotherms.

The discrepancies for the pure component carry over into the mixture case.

Interestingly we also see in Fig. 8 that the IAS theory and the simulations under predict the experimental methane adsorption. Figure 9 shows the adsorbate composition versus bulk composition at fixed pressure. The agreement between simulations and both versions of the IAS theory is very good. The experimental results, on the other hand, show a somewhat lower selectivity for ethane than the simulations or either versions of IAS theory. This is consistent with the under prediction of the experimental methane adsorption by the simulations and IAS theory shown in Fig. 8. Figures 10–14 show corresponding results for a higher temperature of 301.4 K. The conclusions are similar to those from the comparisons shown in Figs. 7–9. However the discrepancy between the methane adsorption determined experimentally and the simulation results is now significantly larger and increases with increasing pressure.

The discrepancies between the methane adsorption predicted by both version of IAS theory and the simulations and the experimental data require some explanation. One possibility to consider is that our model of activated carbon may give rise to intrinsically more ideal behavior for mixtures than real BPL carbon. A more atomistic model (Acharya et al., 1999) might give rise to more energetic heterogeneity and this might make mixture adsorption more nonideal. It is also worthwhile to make a thermodynamic consistency check of the adsorption results from both simulation and

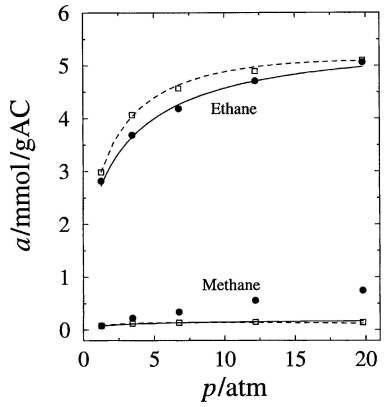

Figure 10. Same as Fig. 7 but for $T = 301.4$ K.

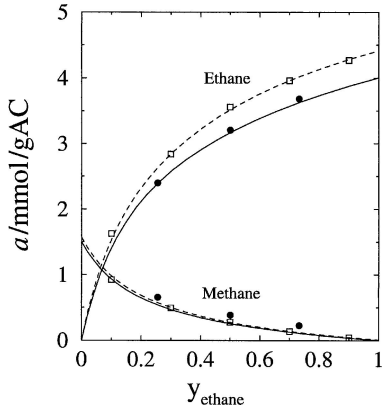

Figure 11. Same as Fig. 8 but for $T = 301.4$ K.

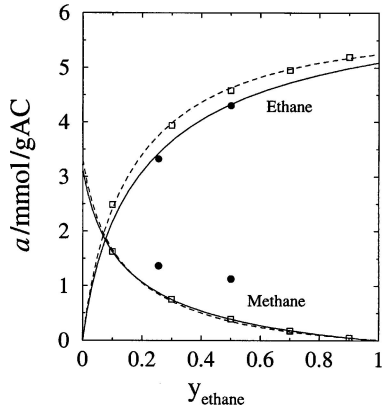

Figure 12. Same as Fig. 8 but for $T = 301.4$ K and $P = 13.6$ atm.

experiment. Thermodynamic consistency of isobaric binary adsorption data can be checked by the intersection rule (Valenzuela and Myers, 1989). The intersection rule requires that at constant T and P any pair of thermodynamically consistent *x-y* curves cross

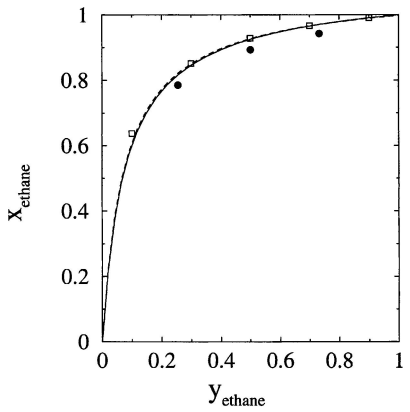

Figure 13. Same as Fig. 9 but for $T = 301.4$ K.

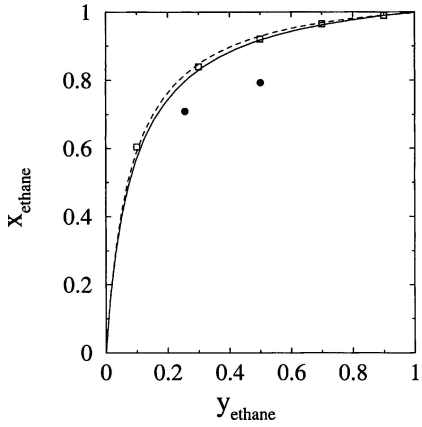

Figure 14. Same as Fig. 9 but for $T = 301.4$ K and $P = 13.6$ atm.

at least once in the region $0 < x < 1$. Figures 9, 13 and 14 show that the *x-y* composition curves indicate that the IAS theory curves based on the pure component simulation isotherms intersect the mixture simulation results. On the other hand there is apparently no intersection between the experimental mixture data and the IAS curves which use the experimental isotherms for the pure components, especially for $P = 13.6$ atm. This suggests that the thermodynamic consistency of the experimental data for this system may be subject to question.

4. Conclusions

In this paper we have presented some new GCMC simulation results for ethane and methane adsorption in activated carbon. The model used is an extension of one developed by Segarra and Glandt (1994). We have

simulated the adsorption isotherms for the pure components and compared with experimental data. The agreement is generally good, especially considering the variability of the data between different BPL carbon samples. Similarly the simulation results for binary mixtures agree quite well with experimental data. The simulation data are also accurately described by the IAS theory. One puzzling feature is the discrepancy between the mixture data and both IAS theory and simulation results for the methane adsorption from the mixture, especially at higher pressures. While it is possibility that the experimental system exhibits more non ideality than is captured in our model system, there does appear to be some evidence of thermodynamic inconsistency in the experimental data.

The present study is the initial phase of a project on studying water and water/organic mixture adsorption in activated carbon using the platelet model. By studying ethane and methane adsorption we have sought to establish the basic geometry of the activated carbon model. The present results suggest that on a basic level we have a reasonably good model of activated carbon upon which to build a study of more complex systems. This will be described in a subsequent paper.

Nomenclature

x_{ff}/k	Adsorbate-adsorbate interaction well depth, K
x_{sf}/k	Adsorbate-adsorbent interaction well depth, K
x_{ff}	Adsorbate-adsorbate collision diameter, nm
x_{sf}	Adsorbate-adsorbent collision diameter, nm
P	Bulk pressure, atm
T	Temperature, K
x_i	Mole fractions in the adsorbed phase
y_i	Mole fractions in the bulk phase

Acknowledgments

This work was supported by a grant from the Army Research Office (Grant No. DAAD19-02-1-0384).

References

Acharya, M., M.S. Stranc, J.P. Mathews, J.L. Billinge, V. Petkov, S. Subramoney, and H.C. Foley, "Simulation of Nanoporous Carbons: A Chemically Constrained Structure," *Philosophical Magazine B*, **79**, 1499 (1999).

Allen, M.P. and D.J. Tildesley, *Computer Simulation of Liquids*, Clarendon Press, Oxford, 1987.

Bandosz, T.J., M.J. Biggs, K.E. Gubbins, Y. Hattori, T. Iiyama, K. Kaneko, J. Pikunic, and K.T Thomson, in *Chemistry and Physics of Carbon*, Radovic, L.R. (ed.), Vol. 28, pp. 41–228, Marcel Dekker, New York, 2003.

Barton, S.S., MJ.B. Evans, and J.A.F. MacDonald, "Adsorption and Immersion Enthalpies on BPL Carbon," *Carbon*, **36**, 969 (1998).

Bradley, R.H. and B. Rand, "On the Physical Adsorption of Vapors by Microporous Carbons," *Journal of Colloid and Interface Science*, **169**, 168 (1995).

Cracknell, R.F., D. Nicholson, and N. Quirke, "A Grand Canonical Monte Carlo Study of Lennard-Jones mixtures in Slit Shaped Pres," *Molecular Physics*, **80**, 885 (1993).

Cracknell, R.F. and D. Nicholson, "Adsorption of Gas Mixtures on Solid Surfaces, Theory and Computer Simulation," *Adsorption*, **1**, 7 (1995).

Finn, J.E. and P.A. Monson, "Prewetting at a Fluid-Solid Interface via Monte-Carlo Simulation," *Physical Review A*, **39**, 6402 (1989).

Franklin, R.E., "Crystallite Growth in Graphitizing and Non-Graphitizing Carbons," in *Proceedings of the Royal Society of London. Series A, Mathematical and Physical Sciences*, **209**, 196 (1951).

Harria, P.J.F., A. Burian, and S. Duber, "High-Resolution Electron Microscopy of a Microporous Carbon," *Philosophical Magazine Letters*. **80**, 381 (2000).

Harris, P.J.F. and S.C. Tsang, "High-Resolution Electron Microscopy Studies of Non-Graphitizing Carbons," *Philosophical Magazine A*, **76**, 667 (1997).

Harris, P.J.F., "Structure of Non-Graphitising Carbons," *International Materials Reviews*, **42**, 206 (1997).

Jensen, C.R.C., N.A. Seaton, V. Gusev, and J.A. OBrien, "Prediction of Multicomponent Adsorption Equilibrium Using a New Model of Adsorbed Phase Nonuniformity," *Langmuir*, **13**, 1205 (1997).

Johnson, J.K., J.A. Zollweg, and K.E. Gubbins, "The Lennard-Hones Equation of State Revisited," *Molecular Physics*, **78**, 591 (1993).

Kaminsky, R.D. and P.A. Monson, "The Influence of Adsorbent Microstructure upon Adsorption Equilibria: Investigations of a Model System," *Journal of Chemical Physics*, **95**, 2936 (1991).

MacDonald, J.A.F., M.J.B. Evans, S. Liang, S.E. Meech, P.R. Norman, and L. Pears, "Chlorine and Oxygen on the Carbon Surface," *Carbon*, **38**, 1825 (2000).

MacDonald, J.A.F. and M.J.B. Evans, "Adsorption and Enthalpy of Phenol on BPL Carbon," *Carbon*, **40**, 703 (2002).

Myers, A.L. and P.A. Monson, "Adsorption in Porous Materials at High Pressure: Theory and Experiment," *Langmuir*, **18**, 10261 (2002).

Myers, A.L. and J.M. Prausnitz, "Thermodynamics of Mixed Gas Adsorption," *AIChE Journal*, **11**, 121 (1965).

Pikunic, J., C. Clinard, N. Cohaut, K.E. Gubbins, J.M. Guet, R.J.M. Pellenq, I. Rannou, and J.N. Rouzaud, "Structural Modeling of Porous Carbons: Constrained Reverse Monte Carlo Method," *Langmuir*, **19**, 8565 (2003).

Reich, R., W.T. Ziegler, and K.A. Rogers, "Adsorption of Methane, Ethane, and Ethylene Gases and Their Binary and Ternary Mixtures and Carbon Dioxide on Activated Carbon at 212–301 K and Pressures to 35 Atmospheres," *Industrial & Engineering Chemistry Process Design and Development*, **19**, 336 (1980).

Segarra, E.I. and E.D. Glandt, "Model Microporous Carbons: Microstructure, Surface Polarity and Gas Adsorption," *Chemical Engineering Science*, **49**, 2953 (1994).

Shing, K.S., "Infinite-Dilution Activity Coefficients from Computer Simulation," *Chemical Physics Letters*, **119**, 149 (1985).

Sircar, S. and R. Kumar, "Column Dynamics for Adsorption of Bulk Binary Gas Mixtures on Activated Carbon," *Separation Science and Technology*, **21**, 919 (1986).

Steele, W.A., *The Interaction of Gases with Solid Surfaces*, Pergamon Press, Glasgow, UK, 1974.

Szczygielska, A., A. Burian, and J.C. Dore, "Paracrystalline Structure of Activated Carbons," *Journal of Physics: Condensed Matter*, **13**, 5545 (2001a).

Szczygielska, A., A. Burian, S. Duber, J.C. Dore, and V. Honkimaki, "Radial Distribution Function Analysis of the Graphitization Process in Carbon Materials," *Journal of Alloys and Compounds,* **328**, 231 (2001b).

Thomson, K.T. and K.E. Gubbins, "Modeling Structural Morphology of Microporous Carbons by Reverse Monte Carlo," *Langmuir*, **16**, 5761 (2000).

Valenzuela, D.P. and A.L. Myers, *Adsorption Equilibrium Data Handbook*, Prentice Hall, New Jersey, 1989.

Vuong, T. and P.A. Monson, "Monte Carlo Simulation Studies of Heats of Adsorption in Heterogeneous Solids," *Langmuir*, **2**, 5425 (1996).

Vuong, T. and P.A. Monson, "Monte Carlo Simulations of Adsorbed Solutions in Heterogeneous Porous Materials," *Adsorption*, **5**, 295 (1999).

Vuong, T., Molecular Thermodynamics of Physical Adsorption in Heterogeneous Solids, Ph. D. Dissertation, University of Massachusetts, Amherst, 1998.

Widom, B., "Some Topics in Theory of Fluids," *Journal of Chemical Physics*, **39**, 2808 (1963).

Wolff, W.F., "The Structure of Gas-Adsorbent Carbons," *Journal of Physical Chemistry*, **62**, 829 (1958).